A R C H I V E S O F M E T A L L U R G Y A N D M A T E R I A L S
Volume 60 2015 Issue 1
DOI: 10.1515/amm-2015-0002

A. CWUDZIŃSKI*

# PIV METHOD AND NUMERICAL COMPUTATION FOR PREDICTION OF LIQUID STEEL FLOW STRUCTURE IN TUNDISH

# METODA PIV I OBLICZENIA NUMERYCZNE DLA PROGNOZOWANIA STRUKTURY PRZEPŁYWU CIEKŁEJ STALI W KADZI POŚREDNIEJ

This paper presents the results of computer simulations and laboratory experiments carried out to describe the motion of steel flow in the tundish. The facility under investigation is a single-nozzle tundish designed for casting concast slabs. For the validation of the numerical model and verification of the hydrodynamic conditions occurring in the examined tundish furniture variants, obtained from the computer simulations, a physical model of the tundish was employed. State-of-the-art vector flow field analysis measuring systems developed by Lavision were used in the laboratory tests. Computer simulations of liquid steel flow were performed using the commercial program Ansys-Fluent®. In order to obtain a complete hydrodynamic picture in the tundish furniture variants tested, the computer simulations were performed for both isothermal and non-isothermal conditions.
*Keywords*: tundish, steel flow, numerical simulation, PIV method

W pracy przedstawiono wyniki symulacji numerycznej i eksperymentów laboratoryjnych opisujących ruch stali w kadzi pośredniej. Analizowanym obiektem była jedno-wylewowa kadź pośrednia przeznaczona do odlewania wlewków płaskich. Do walidacji modelu numerycznego i weryfikacji warunków hydrodynamicznych występujących w analizowanych wariantach zabudowy kadzi pośredniej zastosowano symulacje komputerowe i fizyczny model kadzi pośredniej. W eksperymentach laboratoryjnych do analizy wektorowego pola przepływu zastosowano system pomiarowy firmy Lavision. Symulacje komputerowe przepływu ciekłej stali wykonano programem Ansys-Fluent®. W celu zyskania pełnego obrazu hydrodynamiki ruchu stali w analizowanym obiekcie symulacje komputerowe wykonano dla warunków izotermicznych i nieizotermicznych.

## 1. Introduction

The capability to change the mould dimensions (casting thickness and width) combined with the absence of the bottom (an arbitrary casting length) make the continuous steel casting process the most efficient and flexible method of manufacturing steel semi-finished products. In the Continuous Steel Casting (CSC) technology, the steelmaking ladle, the tundish, the mould and the secondary cooling zone form a single connected vessel in which the liquid steel gradually solidifies [1, 2]. The required stock of metal that flows into the mould is assured by the tundish. In addition, the tundish guarantees the constant mould pouring speed and separates the metal among the moulds in the case of a multi-strand machine. During casting, the refractory lining of the tundish and the slag powders used guarantee the thermal stabilization needed for maintaining the casting temperature required for a given steel grade. Because of the liquid steel residing in the tundish for a specific duration (which is limited by the tundish capacity and the casting speed), it is essential to monitor the tundish operation by analyzing the hydrodynamic conditions [3-5]. The main and side liquid steel stream present in the tundish working space form a complex metal circulation pattern. Hence, modelling of the process of liquid steel flow in the tundish seems to be fully justified. For this purpose, mathematical and physical modelling methods can be successfully used [6-8]. The both research methods are complementary to one another, whereby a number of data are obtained, which describe the phenomena accompanying the flow of liquid steel through the tundish. This paper presents the results of computer simulations and laboratory experiments carried out to describe the motion of steel flow in the tundish. State-of-the-art vector flow field analysis measuring systems developed by Lavision were used in the laboratory tests. Whereas, computer simulations were performed using the Ansys-Fluent® commercial program.

## 2. Characterization of the test facility

The facility under investigation is a single-nozzle tundish designed for casting concast slabs (Fig. 1a). The nominal capacity of the tundish is 30 Mg. Currently, the tundish is furnished with a low dam installed before the bottom step in the stopper rod system area. The height of the low dam is 0.12 m. The dam incorporates two 0.14×0.05 m overflow windows arranged symmetrically relative to the tundish axis.

* CZESTOCHOWA UNIVERSITY OF TECHNOLOGY, DEPARTMENT OF METALS EXTRACTION AND RECIRCULATION, FACULTY OF MATERIALS PROCESSING TECHNOLOGY AND APPLIED PHYSICS, 19 ARMII KRAJOWEJ AVE, 42-200 CZĘSTOCHOWA, POLAND

On the pouring zone side, the tundish is furnished with an overflow trough that protects the tundish against overfilling. The tundish shape resembles a wedge narrowing towards the pouring zone. The submerged entry nozzle discharge orifice and the ladle shroud pouring gate are located in the tundish axis at a distance of 2.915 m from each other. The inner diameters of the openings supplying liquid steel to the tundish and to the mould are identical, being equal to 0.07 m. Figure 1b present the designed dam as shown on a scale of 2:5, which are intended for tests in the physical tundish model. This dam has been positioned perpendicularly to the tundish axis between the side walls. Figures 1c and 1d show the tundish furniture variants on a scale of 1:1, which are intended for numerical simulation. A tundish in the form of virtual models was prepared for numerical simulations using the Gambit 2.4 software program.

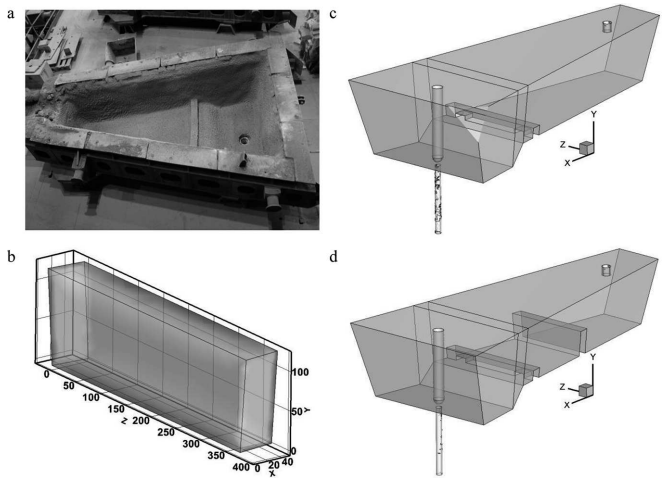


Fig. 1. Test facility: a) industrial tundish, b) physical model of dam, c) virtual model of tundish with low dam, d) virtual model of tundish with high dam

## 3. Testing methodology

The software program Ansys-Fluent® is the world's recognized CFD program that finds application in studies on the motion of steel in the steelmaking technology. The basic mathematical model equations describing the phenomena under examination are as follows:

$$\frac{\partial \rho}{\partial t} + \nabla(\rho u) = 0 \tag{1}$$

$$\frac{\partial}{\partial t}(\rho u) + \nabla(\rho u u) = -\nabla p + \nabla(\bar{\bar{\tau}}) + \rho g \tag{2}$$

$$\bar{\bar{\tau}} = \mu\left[\left(\nabla u + \nabla u^T\right) - \frac{2}{3}\nabla u I\right] \tag{3}$$

$$\frac{\partial}{\partial t}(\rho E) + \nabla(u(\rho E + p)) = \nabla\left(k_{eff}\nabla T - \sum_j h_j J_j + (\bar{\bar{\tau}}_{eff} u)\right) \tag{4}$$

$$E = h - \frac{p}{\rho} + \frac{u^2}{2} \tag{5}$$

$$\rho = 8300 - 0.7105T \tag{6}$$

$$\frac{\partial C_i}{\partial t} + \nabla(-D_i \nabla C_i + C_i u) = 0 \tag{7}$$

where: $C_i$ – concentration of the tracer (kg), $\bar{\bar{\tau}}$ – stress tensor (Pa), $\bar{\bar{\tau}}_{eff}$ – effective stress tensor (Pa), $k_{eff}$ – effective thermal conductivity (W/m·K), I – unit tensor, $\mu$ – viscosity (kg/m·s), $D_i$ – diffusion coefficient of the tracer ($m^2/s$), $\rho$ – density ($kg/m^3$), $\rho_0$ – initial density ($kg/m^3$), u – velocity of the steel flow (m/s), t – time (s), E – energy (J), g – gravitational acceleration ($m/s^2$), p – pressure (Pa), T – temperature (K), h – enthalpy (J), Jj – diffusion flux ($kg/m^2 \cdot s$).

In non-isothermal computation, polynomial density model was employed, which is described by equation 6. For the non-isothermal conditions of steel flow through the tundish, the magnitudes of heat fluxes on particular tundish walls and bottom have been determined to be –2600 $W/m^2$, whereas on the regulator walls –1750 $W/m^2$. The losses on the free metal table surface are –15000 $W/m^2$ [9-17]. The wall condition with zero tangential stress was assumed on the free steel table surface. User defined scalar (UDS) transport equation were used to calculation the motion of the tracer in the liquid steel. For the description of the turbulence of steel flow through the tundish, the Realizable k-$\varepsilon$ turbulence model were adopted. In the Realizable k-$\varepsilon$ turbulence model constants take on the following values: $C_2$ =1.9, $\sigma_k$ =1.0, $\sigma_\varepsilon$ =1.2 [18].

Physical quantities of liquid steel as follows: viscosity 0.007 kg/m·s, heat capacity of steel 750 J/kg·K, thermal conductivity of steel 41 W/m·K. At the inlet tundish, liquid steel inflow of 1.316 m/s was assumed with turbulence kinetic energy 0.0173 $m^2/s^2$ and energy of dissipation rate of kinetic energy 0.065137 $m^2/s^3$. The initial liquid steel velocity corresponded to the sequence of continuous casting of 1.5×0.225 m concast slabs at a speed of 0.9 m/min. The initial liquid steel temperature in the computer simulation was 1823 K.

The system of equations forming the mathematical model of steel flow was solved by the method of control volumes by employing discretization of the second order upwind using the sequential solver. The Semi-Implicit Method for Pressure-Linked Equations-Consistent (SIMPLEC) algorithm was used for the description of the coupling of the pressure and velocity fields in the model being solved. The controlled level of residues was at a level of at least $10^{-3}$. The condition to comply with the impassable $y^+$ parameter values (30÷60) indicating the correct choice of the grid in the wall boundary layers was also respected.

For the validation of the numerical model and verification of the hydrodynamic conditions occurring in the examined tundish furniture variants, obtained from the computer simulations, a physical model of the tundish was employed (Fig. 2). Designed and started up at the Department of Metals Extraction and Recirculation, the physical tundish model enables the measurement of variations in tracer concentration and recording of the visualization of fluid medium motion through the change in tracer colour. The tundish model was made on a scale of 2:5. The tundish model's nominal capacity is 210 litres. According to the similarity criteria, the medium simulating the liquid steel was water, which, at a temperature of 20°C, has the identical kinematic viscosity to that of liquid steel. Studies on the water model were conducted while satisfying the Froude criterion, which ensured that the similarity

between the inertial forces and the gravity forces occurring in the physical model and those prevailing in the metallurgical plant tundish was maintained. The Froude criterion is recommended for simulation of the flow of liquid steel under turbulent motion conditions. Within the conducted "IuventusPlus" project, the physical tundish model was additionally equipped with a 2DPIV (2D Particle Image Velocimetry) vector flow field recording and analysis system supplied by Lavision. Figure 2 shows a camera and a double-cavity laser of a pulse energy of 200 mJ and a wavelength of 532 nm with an optical light knife system with a light beam propagation angle from 15° to 30°. For the analysis of the vector flow field the DaVis 8 software program with the 2DPIV module was employed. Seeding in the form of 10 mL glass balls of a density of 1100 kg/m$^3$(±50 kg/m$^3$) and an average diameter from 9 to 13 $\mu$m was introduced to the water flowing through the physical model of tundish. The job of the seeding was to fill up the flow fields "cut" with the light knife in the working space of the model. The measurement of flow field in the physical tundish model was started after a period of 8 average water residence times (casting two complete melts during CSC). After attaining a steady flow field in the working space of the physical tundish model, the laser was activated, whose beam passing through the optical system formed a light plane in which glass ball motion trajectories were recorded. The employed glass balls flowed following the flow directions that formed in the examined water stream field. Then the camera was started, which was furnished with a filter adapted to the wavelength emitted by the laser, eliminating any environmental interference during recording.

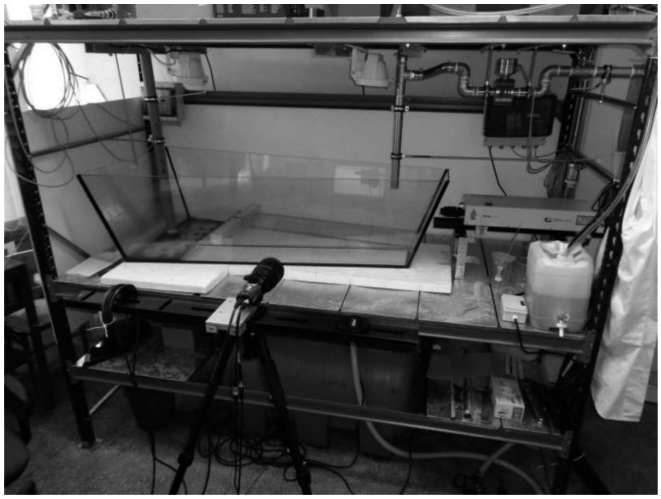

Fig. 2. Physical model of tundish

After the calibration of the size of the flow field to be observed, recording of the vector flow field was started. During a single measurement, 360 frames were recorded, which provided a basis for obtaining the vector flow field. To obtain the complete and reliable picture of the vector flow field for particular tundish furniture variants, the measurement was repeated at intervals of 15-20 minutes. In the next stage of analysis, the recorded glass ball motion was transformed into the vector field form using the 2DPIV module.

## 4. Isothermal simulation

The pattern of liquid steel flow in the tundish is formed by the main feed stream, the sides streams and the reverse streams. Therefore, in order to correctly evaluate the whole of liquid steel motion in the tundish working space, a detailed analysis of the vector field of flow in characteristic locations of the examined facility is needed. To this end, six planes situated in the same locations in all of the examined tundish furniture variants were cut out (Fig. 3a and 4a). Plane no. 1 (P1) intersects the central part of the tundish from the stopper rod system zone to the tundish pouring zone. Plane no. 2 (P2) is positioned in parallel to the longitudinal side wall, encompassing the tundish pouring zone and the stopper rod system zone. Planes nos. 3-6 are the planes transverse to the longitudinal tundish axis. Plane no. 3 (P3) is situated in the axis of the ladle shroud supplying liquid steel to the tundish. While planes nos. 4-6 (P4, P5 and P6) are distant from the plane P3, respectively, by 0.4875 m, 1.4675 m and 2.915 m towards the stopper rod system. This manner of arranging the transverse planes enabled the observation of steel flow directions not only in the pouring zone, but also in the region beyond the pouring zone, the high dam and within the stopper rod system zone.

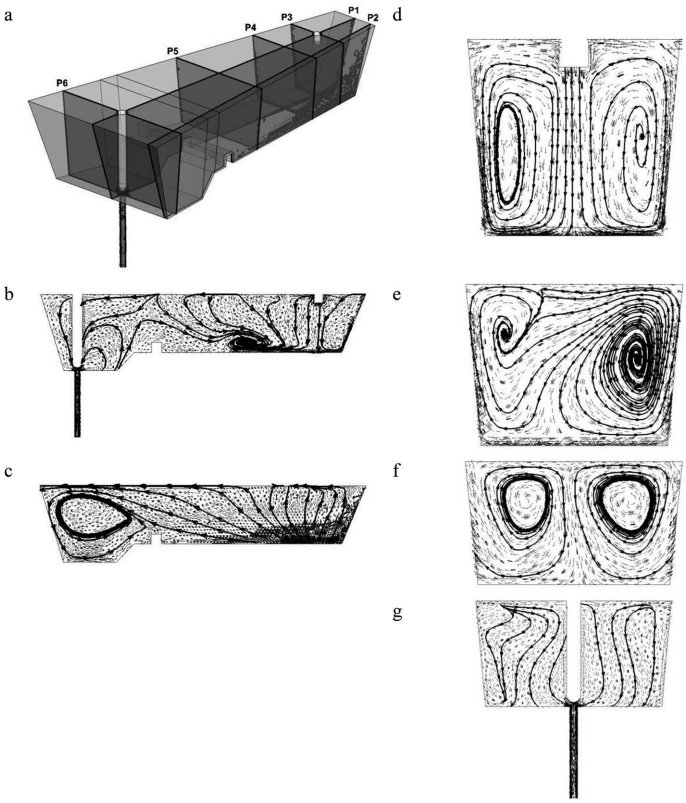


Fig. 3. Fields of liquid steel flow in the tundish with low dam: a) locations of planes, b) central longitudinal plane, c) side longitudinal plane, d) transversal plane no. 3, e) transversal plane no. 4, f) transversal plane no. 5, g) transversal plane no. 6

Figure 3 represents the vector field of liquid steel flow in the low-dam tundish. After flowing into the tundish, the liquid steel hits against its bottom, after which, instead of flowing along the tundish bottom, it moves to the tundish nozzle in the close proximity of the longitudinal side wall, first towards the free surface, and then only in the stopper

rod region it falls down towards the nozzle (Fig. 3c). In the stopper rod system region, at the longitudinal side wall, part of the reverse stream is visible, which, upon the collision with the feed stream, is reversed back towards the stopper (Fig. 3c). When moving towards the longitudinal tundish axis one can see that, in the central tundish part, the reverse stream meets the feed stream only at roughly half the distance between the low dam and the pouring zone, forming a small steel circulation region (Fig. 3b). Initiated in the pouring zone, the circulatory motion from the longitudinal side wall towards the tundish centre evolves in the subsequent regions of the tundish working space (Fig. 3d, 3e and 3f). Consequently, a liquid steel movement descending towards the bottom is visible in the central part of the tundish (Fig. 3b), which is the result of swirling of the steel and the formation of two steel circulation regions between the longitudinal side walls, the bottom and the free surface. It can be seen in Figures 3g and 3e that, in some places, the liquid steel motion relative to the longitudinal axis may take on an asymmetric behaviour, which confirms the dynamism and complexity of phenomena occurring within the bulk of liquid steel. Figure 4 represents the vector field of liquid steel flow in the high-dam tundish.

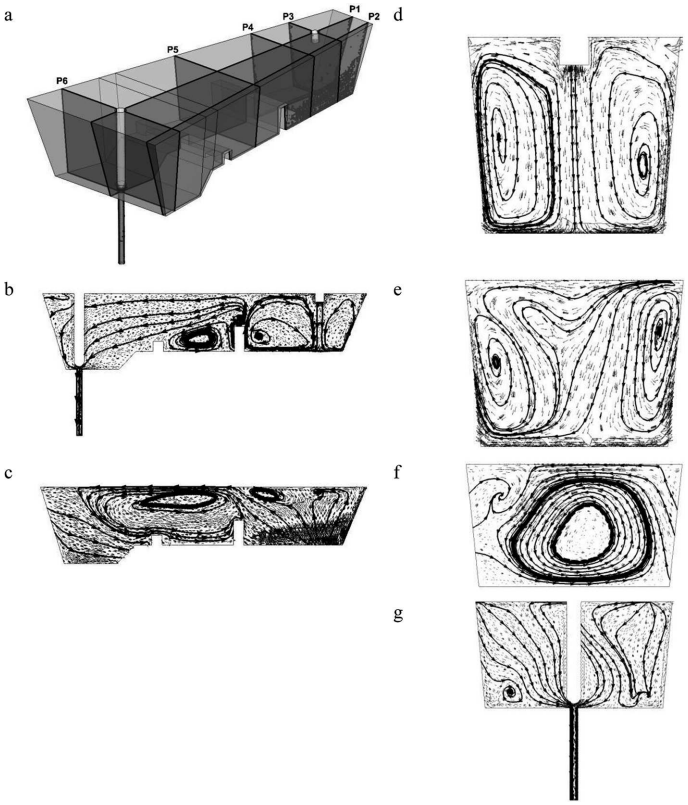


Fig. 4. Fields of liquid steel flow in the tundish with high dam: a) locations of planes, b) central longitudinal plane, c) side longitudinal plane, d) transversal plane no. 3, e) transversal plane no. 4, f) transversal plane no. 5, g) transversal plane no. 6

Upon flowing to the tundish, the liquid steel hits against the bottom and then flows towards the side walls. After reaching the transverse rear wall, the liquid steel flows towards the free steel table surface and then it continues flowing under the table towards the feed stream axis to form a circulation region (Fig. 4b). At the same time, the main feed stream flows in the close proximity of the longitudinal side walls to reach the high dam region (Fig. 4c). It is here that the main stream becomes spit into side streams and reverse streams. The side streams form the circulation region observed in Figure 4c. The reverse streams circulate in the central tundish part between the high dam and the tundish pouring zone. Whereas, the main feed stream flows towards the longitudinal tundish axis, next it is pushed up by the dam towards the free surface, and then it starts falling down on its way to the nozzle (Fig. 4b). In the pouring zone, hydrodynamic conditions similar to those occurring in the low dam-tundish are observed (Fig. 4d). As a result of the main feed stream heading for the central tundish part, a large steel circulation region forms in the longitudinal side wall region beyond the high dam, which is caused by the reverse streams. An interesting phenomenon is observed in the region between the low and high dams, whereby part of the main feed stream is reversed to form reverse streams creating a large steel circulation region in the transverse plane. Upon reaching the front side wall, part of the stream forms reverse streams, and the other part flows on to the tundish nozzle (Fig.4b and 4g).

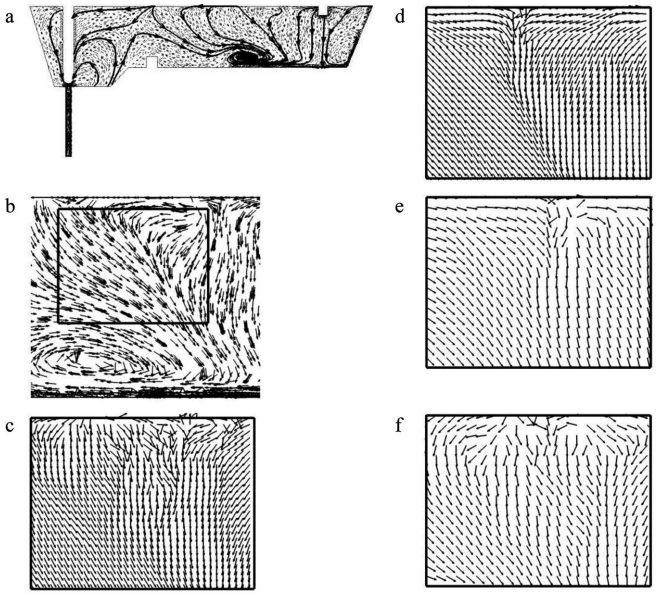


Fig. 5. Fields of liquid steel and water flow in the tundish with low dam: a) numerical simulation – central plane, b) numerical simulation – analysis zone, c) PIV – trial no. 1, d) PIV – trial no. 2, e) PIV – trial no. 3, f) PIV – trial no. 4

The numerical model was verified using the PIV method which was used during simulation in the physical tundish model. The measurements of the vector flow field in the physical model of the examined facility were carried out according to the methodology described in section testing methodology. The plane situated in the central tundish plane (the position of the plane P1), reduced down to the dimensions of 0.525×0.4 m, was chosen for experimental studies. The measurement plane was situated at a height of 0.2625 m above the tundish bottom level and 0.0375 m beneath the liquid steel table. Whereas, in the case of its position relative to the FCD, it was located before the high dam, as seen from the poring zone side, and immediately after the zone of ladle shroud, as seen in the stopper rod system direction. The laboratory

experiment, during which the vector flow fields were determined in the reduced measurement plane by the PIV method was repeated eight times in order to obtain the reliable pattern of flow hydrodynamics in the selected working space of the examined facility. The analysis of the flow pattern in the low-dam tundish, as shown in Figures 5a-f, confirms the good agreement between the results obtained by both examination methods. In both cases, a descending behaviour of the liquid steel and water streams was obtained. Figure 6 represents the vector fields of flow in the tundish with a high dam. In the analyzed region, a liquid steel motion towards the free surface was recorded for the measurement plane, which transforms itself into a reverse flow directed towards the pouring zone (Fig. 6b). A similar flow pattern was obtained in physical simulations (Fig. 6c-f).

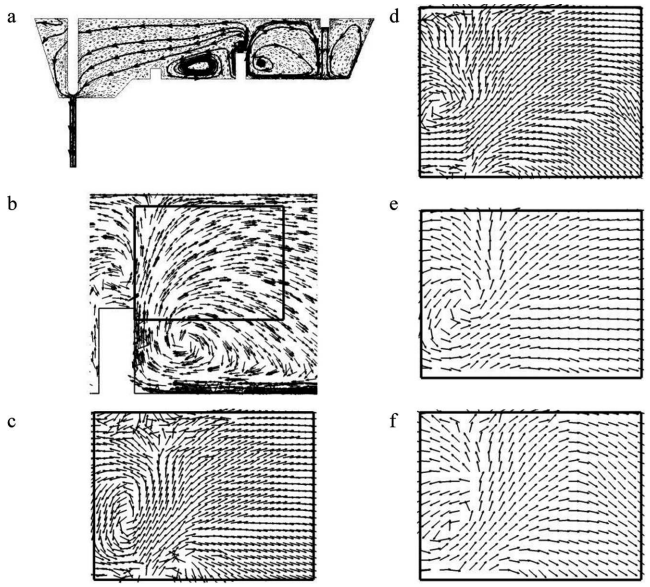


Fig. 6. Fields of liquid steel and water flow in the tundish with high dam: a) numerical simulation – central plane, b) numerical simulation – analysis zone, c) PIV – trial no. 1, d) PIV – trial no. 2, e) PIV – trial no. 3, f) PIV – trial no. 4

## 5. Nonisothermal simulation

Figure 7 represents the maps of vector flow fields and a liquid steel temperature field in the central plane (P1) for two of the tundish furniture variants under analysis. In the tundish with a low dam, a vertical stratification of the temperature field occurs in the central part (Fig. 7c). By contrast, installing a high dam in the tundish results in a horizontal stratification of the steel temperature isolines in the region between the low and the high dam (Fig. 7d). In the propose tundish furniture variants, reverse streams which flow in the lower liquid steel volume and feed streams flowing immediately beneath the steel table surface can be distinguished in the central part of the tundish. In the case of the low-dam tundish, the circulation occurs roughly in the mid-distance between the pouring zone and the low dam. In turn, installing a high dam in the working space causes a circulation to occur before the dam, on the pouring zone side.

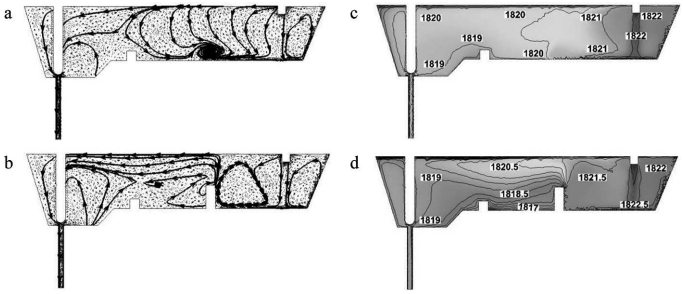


Fig. 7. Fields of liquid steel flow and temperature on the central plane: a) velocity vectors, c) temperature – tundish with low dam, b) velocity vectors, d) temperature – tundish with high dam

Figures 8-9 illustrate liquid steel vector flow and temperature fields in the transverse planes (P3-P6) for the tundish furniture variants considered in the design. In all of the tundish furniture variants, good thermal homogenization was achieved in the pouring zone. In the P4 plane in the high-dam tundishes, lower difference at liquid steel temperature values were recorded. Figures 8g-9g represent the liquid steel temperature fields in the plane P5. The warmer regions located in this plane characterize the zones through which the main feed stream flows up to the stopper rod. In the stopper rod system zone, independently of the tundish furniture variant, a similar distribution of liquid steel temperature isolines was observed (Fig. 8h and 9h). When examining the vector flow fields in the pouring zone,

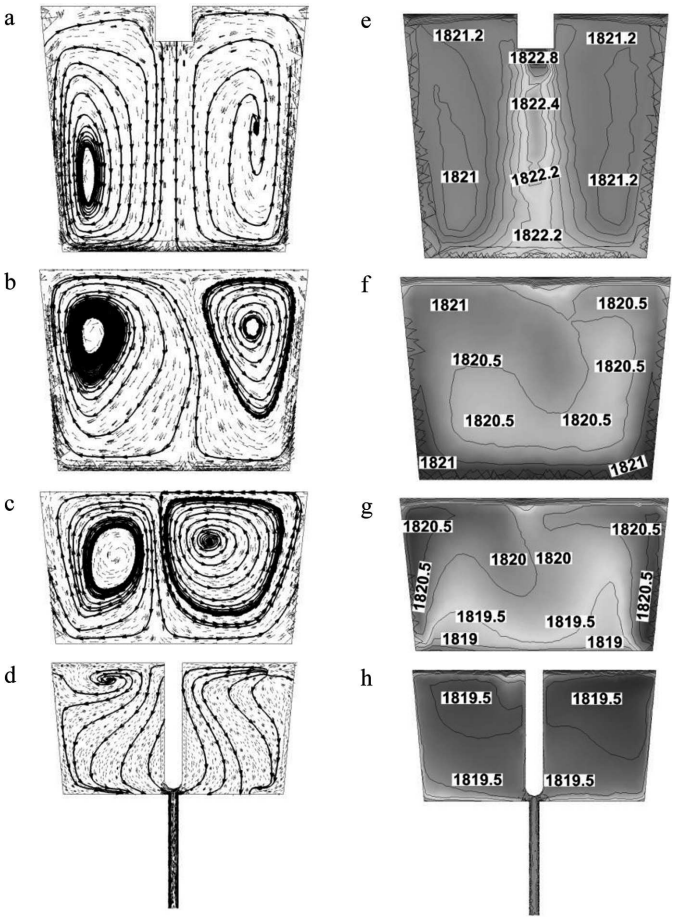


Fig. 8. Fields of liquid steel flow and temperature in the tundish with low dam: a), e) transversal plane no. 3, b), f) transversal plane no. 4, c), g) transversal plane no. 5, d), h) transversal plane no. 6

main patterns can be distinguished. In the tundishes without flow control devices in the pouring zone, liquid steel circulation takes place on either side of the feed stream between the bottom, the side walls, the free surface and the stream axis (Fig. 8a and 9a). In the P4 plane, a liquid steel movement towards the bottom, because no reverse flow occurs in this part of the tundish (Fig. 8b and 9b). In addition, in all tundish furniture variants, steel circulation regions have been located between the longitudinal tundish axis and the side walls (Fig. 8b and 9b). The greatest variety in flow pattern between successive tundish working space furniture variants was observed in the P5 plane. The location of the P5 plane in the low dam region enables the observation of the effect of liquid steel temperature on the formation of steel motion hydrodynamics, whereby, at a distance of 2 m from the pouring zone, the inertial forces diminish, while convective forces start predominating. In the stopper rod system zone, regardless of the furniture type used, the distribution of liquid steel stream flow directions is similar, being distinguished by a pattern descending towards the bottom and the nozzle (Fig. 8d and 9d).

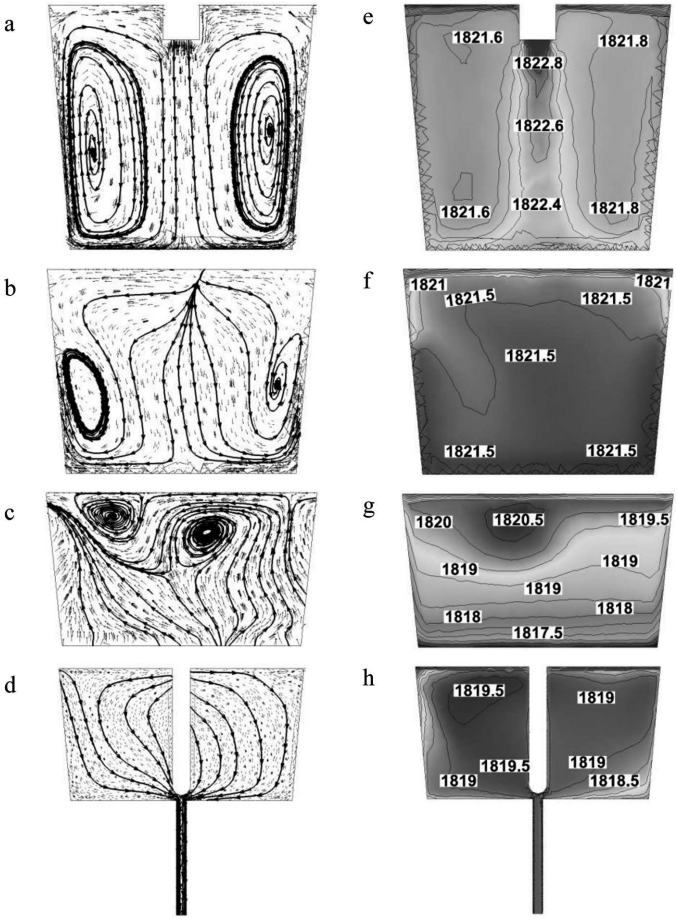


Fig. 9. Fields of liquid steel flow and temperature in the tundish with high dam: a), e) transversal plane no. 3, b), f) transversal plane no. 4, c), g) transversal plane no. 5, d), h) transversal plane no. 6

Having available the hydrodynamic pattern of steel flowing in the tundishes according to successive furniture variants, being formed under either isothermal or non-isothermal conditions, the differences that occur in the working space due to the differentiation of the liquid steel temperature field can be evaluated. Except for the tundish furnished with the low dam, inducing non-isothermal condition during the flow of liquid steel through the tundish, had the effect of modifying the flow pattern in the central part of the examined facilities. In the high-dam tundish variant, the steel circulation region observed beyond the high dam on the stopper rod system side disappears. In the pouring zone of the tundishes in the furniture variants under examination, no significant differences occurred between the steel flow patterns computer for isothermal and non-isothermal conditions. In the zone located beyond the influence of the feed stream, first differences in flow pattern between isothermal and non-isothermal simulations start to reveal themselves. In the high-dam tundish, an ascending motion from the bottom to the free surface occurred in the examined region (Fig. 9c).

## 6. Summary

From the performed computer simulations and laboratory experiments (physical modeling) it can be found that:

- The high dam and low dam positively influence the flow of liquid steel not only in the zone directly affected by them, but also in the remaining regions of the tundish working space;
- the Realizable k-$\varepsilon$ model proposed for the computer simulations of liquid steel flow correctly reflects the vector fields of liquid steel flow occurring in the examined tundish furniture variants;
- the non-isothermal conditions occurring during continuous steel casting will definitely influence on the hydrodynamic pattern forming in the tundish.

**Acknowledgements**

The research work has been financed from the budget resources allocated to research in the years 2012-2013 in the framework of the IuventusPlus programme.

REFERENCES

[1] T. Telejko, Z. Malinowski, M. Rywotycki, Archiv. Metall. Mater. **54**, 837 (2009).
[2] M. Rywotycki, K. Miłkowska-Piszczek, L. Trębacz, Archiv. Metall. Mater. **57**, 385 (2012).
[3] A. Cwudziński, J. Jowsa, Archiv. Metall. Mater. **53**, 750 (2008).
[4] P. Macioł, J. Gawąd, D. Podorska, Archiv. Metall. Mater. **52**, 105 (2007).
[5] L. Sowa, A. Bokota, Archiv. Metall. Mater. **57**, 1163 (2012).
[6] J. Falkus, J. Lamut, Archiv. Metall. Mater. **50**, 709 (2005).
[7] K. Michalek, K. Gryc, M. Tkadleckova, D. Bocek, Archiv. Metall. Mater. **57**, 291 (2012).
[8] K. Janiszewski, Archiv. Metall. Mater. **58**, 513 (2013).
[9] S. Chakraborty, Y. Sahai, Metall. Mater. Trans. B **23B**, 153 (1992).
[10] R.D. Morales, S. Lopez-Ramirez, J. Palafox-Ramos, D. Zacharias, ISIJ Int. **39**, 455 (1999).
[11] Y. Miki, B.G. Thomas, Metall. Mater. Trans. B **30B**, 639 (1999).
[12] M.A. Barron-Meza, J. De J. Barreto-Sandoval, R.D. Morales, Metall. Mater. Trans. B **31B**, 63 (2000).

[13] S. Lopez-Ramirez, J. De J. Barreto, J. Palafox-Ramos, R.D. Morales, D. Zacharias, Metall. Mater. Trans. B **32B**, 615 (2001).
[14] R.D. Morales, S. Lopez-Ramirez, J. Palafox-Ramos, D. Zacharias, Ironmaking Steelmaking **28**, 33 (2001).
[15] R.K. Singh, A. Paul, K. Ray, Scand. J. Metall. **32**, 137 (2003).
[16] S. Lopez-Ramirez, J. De J. Barreto, P. Vite-Martinez, J.A. Romero Serrano, C. Duran-Valencia, Metall. Mater. Trans. B **35B**, 957 (2004).
[17] L. Zhang, Steel Res. **76**, 784 (2005).
[18] T.-H. Shih, W.W. Liou, A. Shabbir, Z. Yang, J. Zhu, Comput. Fluid **24**, 227 (1995).

*Received: 18 July 2013.*